In Vivo Channel Characterization for Dengue Virus Infection

Saswati Pal
Indian Institute of Technology
Kharagpur, India
saswatipal@iitkgp.ac.in

Nabiul Islam
TSSG, Waterford Institute of Technology
Ireland
nislam@tssg.org

Sudip Misra
Indian Institute of Technology
Kharagpur, India
smisra@sit.iitkgp.ernet.in

Sasitharan Balasubramaniam
TSSG, Waterford Institute of Technology
Ireland
sasib@tssg.org

ABSTRACT

Dengue, a mosquito-borne viral disease, poses a global threat owing to the unavailability of any specific therapeutics. Since prevention is only restricted to vector control, a clear understanding of Dengue Virus *(DENV)* transmission within an infected host is essential. The dynamics of *DENV* transmission in-vivo addressed in the light of molecular communication paradigm is promising in providing crucial information accounting for disease control and the clearance of virus infection. In this work, we model the dengue virus transmission inside the body from the point of mosquito bites to the targeted organs as a communication system. Based on the physiological processes involved in the transmission of dengue virus through the layers of skin and vascular system, we identify and propose a channel model. By considering the dynamics of virus transmission through the channel, we analyze and calculate different channel phenomena, such as path loss and channel noise, and obtain an analytical expression for the capacity of the proposed channel model. The uncertainty in signal transmission is modeled and evaluated owing to the innate and adaptive immune response in the channel. We performed in-silico experiments for validation and provided numerical analysis for the channel characteristics. Our analysis revealed that the attenuation offered in the cutaneous channel does not result in significant signal loss. It is observed that the variation in channel capacity is not substantially affected by the symbol probabilities.

KEYWORDS

Dengue virus, in vivo transmission, channel model, path loss, capacity analysis, information theory

ACM Reference Format:
Saswati Pal, Nabiul Islam, Sudip Misra, and Sasitharan Balasubramaniam. 2019. In Vivo Channel Characterization for Dengue Virus Infection. In *Proceedings of NanoCom '19: ACM International Conference on Nanoscale Computing and Communication (NanoCom '19).* ACM, New York, NY, USA, 7 pages. https://doi.org/10.1145/nnnnnnn.nnnnnnn

NanoCom '19, September 25–27, 2019, Dublin, Ireland

ACM ISBN 978-x-xxxx-xxxx-x/YY/MM…$15.00
https://doi.org/10.1145/nnnnnnn.nnnnnnn

1 INTRODUCTION

Nanomedicine provides a platform for significant development in disease monitoring, in-vivo drug delivery, therapeutic and diagnostic techniques, and can be realised via nano-networking and molecular communication. Dengue is one of the globally recognized critical and threatening diseases due to its pandemic nature in recent decades. It is an *Aedes* mosquito-borne infection transmitted to humans by Dengue virus *(DENV)* belonging to the *Flaviviridae* family. Dengue spread by five different serotypes, *DENV-1, DENV-2, DENV-3, DENV-4,* and *DENV-5* from the virus family. These serotypes are antigenically distinct and produce a unique immune response to the infection in the host body. *DENV* approximately infects around 50 million people world-wide per year [1]. The core of Dengue virus is a positive single-stranded RNA genome inside a protein, encapsulated by a lipid envelope. The genome functions as mRNA (Messenger RNA) and convey genetic information from DNA to any cell via vesicles for genome synthesis. The spread of multiple dengue serotypes from one organism to another increases the plausibility of genetic transformation. These RNA viruses have higher genetic recombination rate leading to the emergence of new virus serotype [2]. The continuous process of concurrent infections with distinct dengue virus serotypes and genetic transformations over the years lead to novel challenges in dengue control. Any dengue vaccine is effective only when it provides immunity against all the infectious variants of dengue serotype.

Currently, the vaccine available to treat dengue infection is not effective as the immunity against one serotype does not protect the host from other four serotypes. Moreover, being immune to one virus serotype while subsequently getting infected with another serotype triggers even more critical disease manifestations [3]. Also, a seronegative individual getting vaccine for immunisation develops a risk for subsequent severe dengue infection. According to WHO, a prior screening test and surveillance of infections from similar virus family is recommended before reaching out for vaccination [4]. Even if a vaccine is likely to be immunogenic to all the five serotypes identified, it may not be able to offer immunity against additional *DENV* serotypes which are in mutation cycle. The further discovery of such serotype would raise a risk in the available dengue vaccine. The ever-increasing mortality rate due to the spread of infectious diseases has evoked the exigency for early identification as well as progression of the illnesses. By recognizing the aetiology of dengue fever and the plausible steps involved in its pathogenesis, the early detection of the critical disease is possible. *DENV* plays a diverse

role in the clinical manifestations. Since vaccination is yet not an effective tool to combat dengue, identifying the pathways of circulating virus serves to be beneficial. Moreover, detecting the underlying mechanisms leading to *DENV* infection aids in understanding the disease and its pathology. This would assist in accurate diagnosis, developing methods to counteract dengue, and producing antiviral drug.

An essential question is whether we can model the propagation behaviour of *DENV*, and in particular its impact as it propagates through various sub-systems of the human body. In this paper, we propose the use of molecular communications to model the propagation behaviour of *DENV* inside a human body. Our aim is to define the propagation behaviour through the use of communication metrics, such as an analytical channel model that can establish the propagation from the skin to the cellular compartments or organs. Based on the spread of the virus along different paths and limitations faced from the immune system, we derive the path loss model. Our molecular communication model links the spreading of the virus to the signal transmission, where the immune response is abstracted as the attenuation induced during transmission, while the target sites serve as the receiver.

1.1 Contribution

The following list constitutes the major research contributions of this paper:

- *Modeling dengue transmission as an end-to-end abstraction of molecular communication channel*: We propose a communication channel model for *DENV* transmission in-vivo. The proposed channel model maps biological processes to major elements of a communication system. We evaluated the channel on the basis of biomolecular kinetic processes.
- *Determining the influence of the channel on signal transmission*: We characterize a path loss model for signal transmission based on the effect of host's physiological response. Also we approximate a noise model for the channel.
- *Evaluating information theoretic-analysis of the channel*: We analytically evaluate the capacity of the channel obtaining the expression for channel transition probabilities.

2 RELATED WORK

Major efforts in the closely related area of *DENV* transmission are focused on the epidemiological models of disease transmission in human and vector populations. The relatively few works towards dengue infection considered monocytes as the only target for infection [5], while assuming constant production rate for the same. However, it is observed that varying rate of monocyte production contributes to viral infection [6]. Few other works considered role of antibodies [7] and antiviral therapy [8] during viral infection.

Recent attempts in exploring dengue infection typically deals with the aspects of virology and immunology. Our work is distinct in respect of modeling virus transmission as a communication system with molecular communication mode. Few works related to drug delivery systems model the channel through the molecular communication paradigm [9, 10]. The proposed model maps the physiological and bio-molecular processes into the communication elements. We develop the channel model to identify the dynamics in signal transmission towards multiple receivers and characterize the channel.

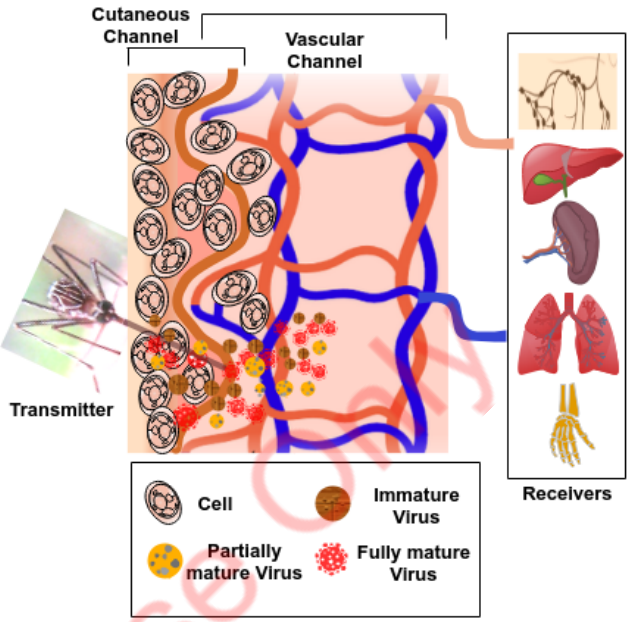

Figure 1: Overview of the system

3 *DENV* TRANSMISSION MODEL

We model the transmission of *DENV* within a host body as a communication system. The source for signal of the system is generated by the event of biting into human with infected female mosquito. By using the direct cell-to-cell transmission strategy, *DENV* propagates through the cells and vascular network to the blood cells, and reaches various organs. The pathogenesis of dengue modeled as a communication system which is shown in Fig. 1, broadly includes the following communication elements:

- **Transmitter**: It represents the proboscis of the infected female mosquito containing dengue virus along with the saliva that enter the skin in search of blood. The common source for signal transmission in our conceptualized system is the point when the mosquito bites the skin of a human and injects the virus into the body. We assume only one serotype of dengue virus is injected. The source *signal*, denoted by $V(t)$, composed of three distinct virulence of the serotype, which is partitioned into three mutually exclusive sets, $V(t) = V_{im}(t) \cup V_{pm}(t) \cup V_{fm}(t)$ representing immature, partially mature and fully mature virus, respectively, which differs from each other based on their maturation level. The V_{im} and V_{pm} fuses into the host cells to undergo subsequent steps of maturation and cleaving to transform into a V_{fm}. Typically, during each biting, around 10^4 to 10^6 of virus particles capable of infection gets injected into the host body [11].
- **Channel**: During several biting by the mosquito, majority of virus escapes into the epidermis and dermis layers of the skin, while relatively small amount of virus reaches the bloodstream

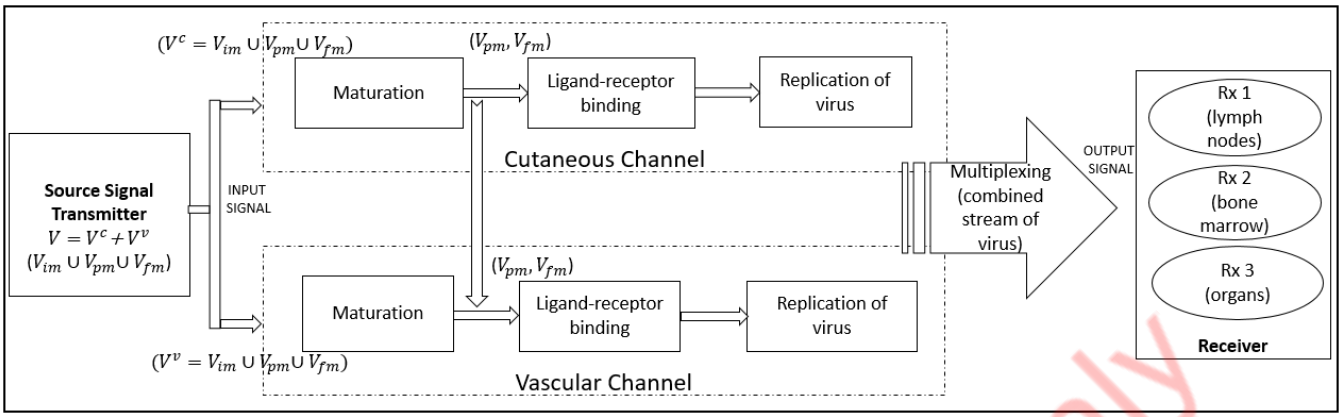

Figure 2: Block diagram of communication system representing dengue transmission

[1]. Thus the channel can be categorised into two subchannels: (1) Cutaneous, which consists epidermis and dermis layers of the skin cells and (2) Vascular, which consists blood vessels for signal transmission.

- **Receiver**: It is the set of sites such as, lymph nodes, bone marrow, and organs (liver, spleen, and lung) [12], which receives virus and gets affected with dengue. In this model, the strength of the signal at the receiver is defined as the time-varying number of virus particles present within the multiple receivers.

The *DENV* transmission in human body is abstracted as a communication model as conceptualized in Fig. 2. The abstracted processes are further discussed in detail in following subsections.

3.1 Channel Modeling

The modeled communication channel is categorised into two subchannels. A proportion of the transmitted signal, V^c goes into the cutaneous channel whereas the remaining of it V^v goes into the vascular channel. Both the proportions from the source signal V are transmitted simultaneously over the subchannels. A part of the transmitted signal along the cutaneous channel escapes into the vascular channel after maturation. The signals from both the subchannels are multiplexed in the bloodstream before it reaches the multiple receivers.

(1) Cutaneous Channel Typically, consists of langerhans cells (LCs) and epithelial cells (ECs) from epidermis while the dendritic cells (DCs), tissue macrophages (MPs), mast cells (MCs), and fibroblasts in dermis for cutaneous route of signal transmission [12].

(2) Vascular Channel The vascular route consists of interconnected blood and lymph vessels which includes the lymphocytes, monocytes, and macrophages of WBC, and platelets to transmit signal [12, 13].

Since only selective mature virus has the ability to invade and replicate inside host cells, the transmitted signal propagating over both the subchannels undergo three major processes – **maturation**, **ligand-receptor binding** and **replication of virus**.

3.1.1 Maturation. The transmitter transmits a set of information particles $\{V_{im}, V_{pm}, V_{fm}\}$ into the channel. Along the channle, the immature and partially mature virus particlesconvert to fully mature virus particles in furin-dependent environment. We consider the immature virus convert into partial mature with a rate of δ_{im} and eliminated with a phagocytic rate ρ_{im}. In a similar manner, the partially mature virus convert and eliminate with rates δ_{pm} and ρ_{pm}, respectively whereas the mature virus is transmitted along the channel. Thus the maturation of virus in channel is quantified with the following differential equation:

$$\frac{dV_{im}}{dt} = \jmath \cdot V_{im} - (\delta_{im} + \rho_{im})V_{im} \tag{1}$$

$$\frac{dV_{pm}}{dt} = \jmath \cdot V_{pm} + \delta_{im}V_{im} - (\delta_{pm} + \rho_{pm})V_{pm} \tag{2}$$

$$\frac{dV_{fm}}{dt} = \jmath \cdot V_{fm} + \delta_{pm}V_{pm} - \rho_{fm}V_{fm} \tag{3}$$

where $\jmath$ is the virus injection rate and ρ_{fm} is the elimination rate of V_{fm} via phagocytosis.

3.1.2 Ligand-receptor binding. The virus is passed through the channel only when it get access to the host cell via binding. For a virus particle to enter into the intracellular environment, the particle's ligands must bind to the surface receptors of host cell. Thus, binding can be abstracted as filtering, following which the particles enter into the host via endocytosis and initiate replication. The process is majorly influenced by recognition and attachment between viral surface ligand and cellular surface receptor molecules which are usually electrostatic in nature. The overall process is facilitated by the factors such as the number of virus ligands n_l, number of receptors n_r, and binding rate r. The ligand-receptor interaction is basically the intermolecular attraction exploited by the biomolecular kinetics, where the number of ligand-receptor complexes n_c formed is given by [14]

$$\frac{dn_c}{dt} = rn_l(n_r - n_c) \tag{4}$$

The binding site where the ligand-receptor comes into physical contact is referred to as interface. This interface often witnesses defensive strategies, such as the random fluctuation in density of the fluidic environment characterized by *Gaussian noise* triggering the receptor diffusion. By incorporating the noise model [14], the effective number of receptors is given as $n_r(t) = \bar{n_r} + \sigma\xi(t)$, where $\bar{n_r}$ is the average number of receptors, σ^2 is the noise intensity, and $\xi(t)$

is the *Gaussian noise*. The number of receptors n_r fluctuate at the interface due to diffusion, thus effecting adversely in the formation of complexes. To account for these noisy effects on the binding, we model n_c utilizing the noise in Eq. (4) as follows:

$$dn_c(t) = rn_l(\bar{n_r} + \sigma\xi(t) - n_c(t))dt - D_r n_c(t)dt \tag{5}$$

where D_r corresponds to the receptor diffusion coefficient. Rewriting Eq. (5) in the differential form, we get the stochastic differential equation as:

$$\begin{aligned} dn_c(t) = rn_l(\bar{n_r} - n_c(t))dt - D_r n_c(t)dt \\ + rn_l\sigma\xi(t)dt \end{aligned} \tag{6}$$

where Gaussian noise being stationary has the mean term, $\overline{\xi(t)} = 0$. By solving Eq. (6) the solution is obtained as follows:

$$\begin{aligned} n_c(t) = e^{-(rn_l+D_r)t} \int_0^t \{rn_l\bar{n_r} + rn_l\sigma\xi(u)\} \\ e^{(rn_l+D_r)u}du \end{aligned} \tag{7}$$

3.1.3 Replication of virus. The endocytosis and replication of V, which produces more virus offsprings, are speculated as amplification of the signal. After entering into the host cell, V_{fm} fuses with the endosomal membrane releasing its nucleocapsid containing single-stranded RNA into the cytoplasm. Following a series of steps at the endoplasmic reticulum (ER), the viral RNA is replicated, amplified, and formed into numerous V_{im} to appear on the ER surface. These are then transported into the trans-Golgi network to release V_{fm} thereby amplifying the signal [15]. At time $t = 0$, considering closed group of N number of cells at the target site, N_{sc} denotes the number of cells susceptible to receive the virus, while N_{ic} are the cells already invaded by the virus. We assume there are no further virus injection from outside into the closed group during the course of in-vivo virus transmission. In an interacting environment, the population growth of V_{fm} and N_{sc} forms a backdrop for the *predator-prey model*. Considering susceptible host cells N_{sc} as the prey and mature virus particles V_{fm} as the predator, the corresponding densities after amplication is modeled as:

$$\frac{dN_{sc}}{dt} = (\alpha - \beta)N_{sc} - \varphi N_{sc}V_{fm} \tag{8}$$

$$\frac{dV_{fm}}{dt} = \upsilon_e\left(1 - \frac{V_{fm}}{C_e}\right) + \gamma N_{sc}V_{fm} - \mathfrak{d}V_{fm} \tag{9}$$

where α represents the growth rate of the susceptible host cells in absence of virus particles, β denotes the transition rate from susceptible cells to infected cells, and φ stands for predation rate upon prey. The transition rate determined by the probability of successful binding is $\beta = P(b)$. The parameter υ_e denotes the engulfing or endocytic rate, and C_e represents the engulfing capacity of the host cell given the fact that diameter of host cell is in μm while that of a virus particle is in nm, and the time t is measured in microseconds. The γ represents the growth rate of V_{fm} inside the host cell depicting the amplification (virus replication) rate and $\mathfrak{d}$ be its (predator) death rate. The transmission of *DENV* in the channels do not follow an entry-exit route from any cell rather it scatter to the neighboring cells following a *lateral transmission* [11]. The virus particles replicate and undergoes maturation inside the host cells and newly formed virus cells are released which infects the nearby cells. The lateral spread of infection accounts for the *bandwidth* of the signal. Thus the bandwidth is determined by the number of infected cells N_{ic} in the channel at time t. Thus the signal bandwidth can be obtained from the following equation:

$$\frac{dN_{ic}}{dt} = rV_{fm}N_{sc} - \kappa N_{ic} \tag{10}$$

where r denotes the ligand-receptor binding rate while κ represents the rate at which the infected cells die.

3.2 Noise Characterization

It has been observed that vitamin D synthesis in cutaneous environment modulates immune response, decreasing the number of virus transmitted [16] thereby reducing the signal strength. In our model, the modulation of immune response is characterized as the noise factor that adds uncertainity to the propagation of signal. The signal is lost in the channel and do not reach the receivers. We thus consider Additive white Gaussian noise (AWGN) $\Re(t) \sim \mathcal{N}(0, \sigma_v^2)$ to model the *propagation noise*. Thus the rate of signal propagation affected by noise along the channel is expressed as:

$$\frac{dN_{ic}}{dt} = rV_{fm}N_{sc} - \kappa N_{ic} + \Re(t) \tag{11}$$

where σ_v^2 is the noise intensity.

3.3 Path Loss

3.3.1 Path Loss in Cutaneous Channel. DENV reaches several receiver sites through the bloodstream by utilizing the two channels discussed above. The propagation from the skin to the different receivers witnesses the immune system at each stage triggered by the cells. The path loss is abstracted as the loss of virus particles due to the immune response during propagation along the channel. As the virus invades, the surface receptors produce antigens over the host cells marking the presence of virus particles, which in response triggers the innate immune response in the cutaneous channel. The path loss in cutaneous channel is due to the innate immune response triggered with the production of signaling proteins such as interferons (IFNs) by LCs, chemokines by MCs, and cytokines by the ECs within few hours of infection [15, 17]. The innate attenuation (A_i) dynamics takes into account production and death rates of immune proteins that mediates the cellular adaptive attenuation A_{cel} modeled as follows:

$$\frac{dA_i}{dt} = a_i N_{sc} - i_c A_i A_{cel} - a_r A_i - (V_{im} + V_{pm}) \tag{12}$$

where a_i is the attenuation rate of virus particles depicting the rate of production of immune proteins, i_c represents the production rate of immune cells activated by immune proteins, and a_r is the removal rate of the immune proteins.

3.3.2 Path Loss in Vascular Channel. The increase in innate attenuation activating the adaptive (cellular and humoral) immune system allows for pertinacious attenuation to V_{fm} transmission. The cascade of immune response in the dermal cells stimulates cellular response (T cells, B cells, and natural killer (NK) cells) [15] as well as humoral response (antibodies) [18] accounting for the path loss in vascular channel. For cellular attenuation we assume decay rate to be negligible pertaining to the cytokine storm resulting in abnormal

proliferation of attenuation.

$$\frac{dA_{cel}}{dt} = i_c A_i A_{cel} + a_c N_{sc} - (V_{im} + V_{pm}) \tag{13}$$

where a_c represents proliferation rate of immune cells. Upon activation of immune response around the cells, the fusion of V_{im} and V_{pm} into the host cells gets hindered, which is rendered by the term $V_{im} + V_{pm}$ in Eqs. (12) and (13). The attenuation originating from humoral response (A_{hmr}) is modeled as follows:

$$\frac{dA_{hmr}}{dt} = (\eta - \eta_{th})N_{sc} - A_{hmr}N_{ic} - A_{hmr}V_{fm} \tag{14}$$

where η and η_{th} denotes the production rate of antibodies and threshold parameter that the antibodies must exceed to attenuate the virus. In this case, the factor $A_{hmr}V_{fm}$ accounts for the clearance rate of antibodies by the virus. Thus the total path loss in the vascular channel, which is abstracted through a diffusion model in a fluidic medium is obtained as $A_v = A_{cel} + A_{hmr}$.

4 CAPACITY ANALYSIS

In the modeled channel, the input alphabet consists of a set of three symbols represented as $\{V_{im}, V_{pm}, V_{fm}\}$, whereas the output alphabet consists of two symbols represented as $\{O_{pm}, O_{fm}\}$, as shown in Fig. 3. We consider the input symbols are injected with probabilities

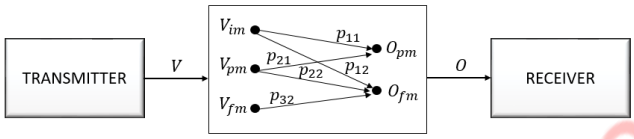

Figure 3: Signal transmission through channel

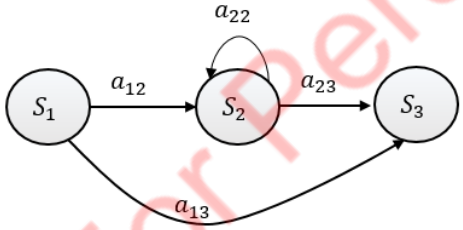

Figure 4: State transition diagram

p_i, p_p, and p_f, respectively. The transition probabilities $p(O_{pm}|V_{pm})$ and $p(O_{fm}|V_{fm})$ are denoted as p_{21} and p_{32} respectively, whereas $p(O_{pm}|V_{im})$, $p(O_{fm}|V_{im})$ and $p(O_{fm}|V_{pm})$ are the transition error probabilities, which are denoted as p_{11}, p_{12}, and p_{22}, respectively. While traversing the channel, the immature virus particles undergo maturation and therefore, they cannot be found at the receiver end. Hence, there are two symbols at the output of the channel: O_{pm} and O_{fm}. Since the fully mature virus particles do not undergo any maturation, the transition probability $p(O_{fm}|V_{fm})$ is $p_{32} = 1$. The dynamics of virus maturity is broadly described by the three major states characterized by – immaturation, partially maturation and fully maturation. The partially mature and fully mature virus are determined by the presence of uncleaved prM (pre-membrane) protein in the former, while cleaved prM in the latter [19]. We consider the dynamics of virus maturity to be represented as a continuous time discrete-state Markov process with aforementioned three states, which are denoted as S_1, S_2, and S_3. The state transition probabilities between the states are denoted as a_{12}, a_{13}, a_{22}, and a_{23}, which are shown in Fig. 4. In state S_1, the immature virus particles fuse with the cell membrane with rate δ_{fn} and enter into the host cells in order to undergo maturation. The states S_2 and S_3 represent the partially maturation and fully maturation of the virus particles, respectively. Thus, we can map the state transition probabilities into the channel's transition error probabilities as $a_{12} = p_{11}$, $a_{13} = p_{12}$, $a_{22} = p_{21}$, and $a_{23} = p_{22}$. The state transition probabilities p_{11} and p_{22} can be obtained from the transition rates for the influx and outflux of V_{im}, V_{pm}, and V_{fm} which is given as follows:

$$p_{11} = \frac{\delta_{im}}{\delta_{im} + \delta_{fn}} \tag{15}$$

$$p_{22} = \frac{\delta_{pm}}{\delta_{pm} + \delta_{im}} \tag{16}$$

where δ_{im} and δ_{pm} are the conversion rates from S_1 to S_2 and from S_2 to S_3, respectively. The rates δ_{im} and δ_{pm} corresponds to the transition rate as discussed in Section 3.1.1. By using the above description of the channel, we get the joint symbol probabilities $p(V_j, O_k)$ as: $P(V_{im}, O_{pm}) = p_{11}p_i$, $P(V_{im}, O_{fm}) = (1 - p_{11})p_i$ $P(V_{pm}, O_{pm}) = (1 - p_{22})p_p$, $P(V_{pm}, O_{fm}) = p_{22}p_p$, and $P(V_{fm}, O_{fm}) = p_f$ where $j \in \{im, pm, fm\}$ and $k \in \{pm, fm\}$. Solving for the output symbol probabilities $p(O_k)$ we get, $p(O_{pm}) = p_{11}p_i + (1 - p_{22})p_p$, and $p(O_{fm}) = (1 - p_{11})p_i + p_{22}p_p + p_f$. The transition matrix for the channel is expressed as:

$$P = \begin{bmatrix} p_{11} & 1 - p_{11} \\ 1 - p_{22} & p_{22} \\ 0 & 1 \end{bmatrix}$$

The mutual information is obtained as follows:

$$\begin{aligned} I(V;O) &= \sum_{o \in O, v \in V} p_{(V,O)}(v,o) \log \left(\frac{p_{(V,O)}(v,o)}{p_V(v)\, p_O(o)} \right) \\ &= -\Big((1 - p_{22})p_p\Big)\, log((1 - p_{22})p_p) - \\ &\Big((1 - p_{11})p_i + p_{22}p_p + p_f\Big)\, log\Big((1 - p_{11})p_i + p_{22}p_p + p_f\Big) \\ &+ p_{11}p_i log(p_{11}) + p_{12}p_i log(p_{21}) + p_{21}p_p log(p_{12}) \\ &+ p_{22}p_p log(p_{22}) \end{aligned} \tag{17}$$

The information-theoretic capacity of the channel with input alphabet V and output alphabet O, which is defined as the maximum mutual information $I(V;O)$ over the symbol probability $p_v \in (p_i, p_p, p_f)$, is given by:

$$C = \max_{p_v} I(V;O) \tag{18}$$

5 NUMERICAL ANALYSIS

We performed in-silico experiments to evaluate the channel performance in terms of signal transmission, attenuation along the

channel, and capacity of the channel. The Python-based simulations are carried out to numerically solve the set of ordinary differential equations defining the proposed cahnnel. The values against the parameters used in the simulation, which are collected from the existing literature [5, 20, 21] are listed in Table 1. In each simulation, a set of 10^4 virus (the value commonly taken for *DENV* based experiment [11]) and 100 susceptible cells in the vicinity are considered in a confined area. In the modeled channel, the time considered is in days depicting the in-vivo transmission of signal. The variation of

Table 1: Simulation Parameters

Parameter	Value
Growth rate of susceptible cells (α)	10
Transition rate of cells (β)	1
Predation rate of virus (φ)	0.002
Replication rate of virus (γ)	20
Production rate of immune proteins (a_i)	4
Production rate of immune cells (a_c)	10
Production rate of antibodies (η)	15

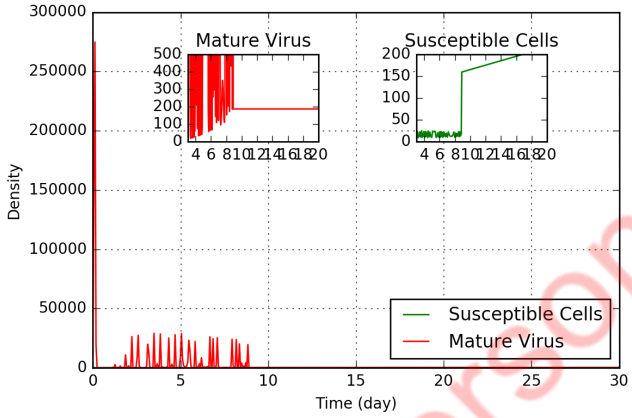

Figure 5: Variation of signal in the channel

signal strength during the transmission along the channel is shown in Fig. 5. We estimated the endocytic rate and engulfing capacity to be 0.8 and 1, respectively, while the death rate of virus was estimated to be 300 with respect to the initial injection of 10^4 virus particles. The signal strength refers to the concentration of virus particles along the channel over the time period measured in days. It was observed that initially the concentration increases and then reaches a fixed value, which is referred to as an equilibrium. However, the concentration of host cells shows a contrast behavior. As the virus continues invading susceptible host cells, the concentration of host cells decreases and then gradually tends to increase with the onset of immune response. The frequency domain representation of the signal is shown in Fig. 6. It was noted that the signal strength decreased gradually with time due to the rapid increase in immune response in both the channels, resulting in the attenuation of the signal as shown in Fig. 7. It was also observed that in the cutaneous channel the signal attenuates in the initial period following injection, while the signal attenuates more in later time in the vascular channel.

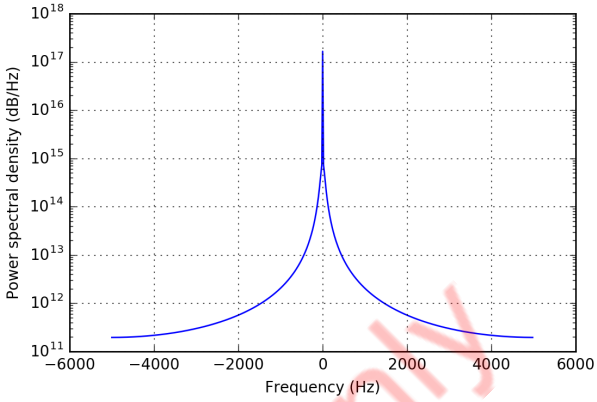

Figure 6: Power spectrum of the signal

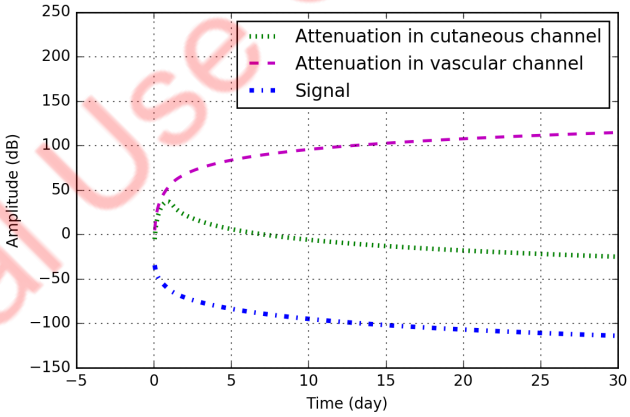

Figure 7: Variation of signal strength and attenuation

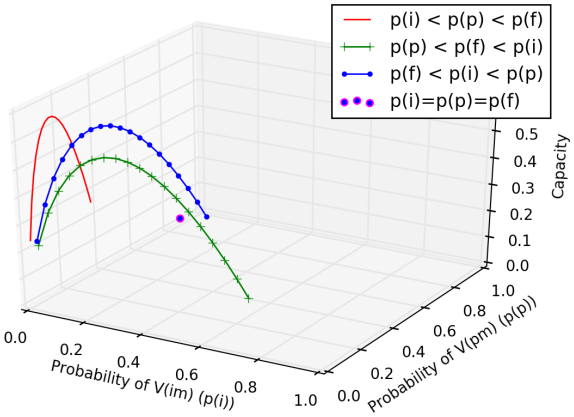

Figure 8: Capacity as a function of symbol probabilities

The signal is stronger initially when the value is close to zero in negative dB scale. The higher the attenuation value, the more the

likelihood of degradation in signal strength. Fig. 8 shows the trend of the channel capacity with the variation of the symbol probabilities with which the virus particles get injected inside human body. It was observed that the value of channel capacity reaches maximum when the condition of symbol probabilities, $p_i < p_p < p_f$, holds. The influence of V_{fm} is found to be greater than its counterparts (V_{im} and V_{pm}) at the receiver. Since all the input symbol has equal probability for $p_i = p_p = p_f$, the capacity is restrained at one point.

6 CONCLUSION

In this work, we proposed an end-to-end communication system for *DENV* proliferation inside a human body. The modeling and analysing provides crucial information on the change in the profile of virus during their transmission which plays key role for the development of novel mechanism to stop the spread of dengue virus. We evaluated the proposed channel model by showing the variation of different channel characteristics with time such as attenuation, signal strength, and the channel capacity. In future, we intend to explore the impact of time-varying channel condition on the achievable maximum rate. We also plan to include noise that the channel encounters in the fluidic environment in order to get in-depth insight of the *DENV* proliferation inside the body.

REFERENCES

[1] Sansanee Noisakran, Nattawat Onlamoon, Pucharee Songprakhon, Hui-Mien Hsiao, Kulkanya Chokephaibulkit, and Guey Chuen Perng. Cells in dengue virus infection in vivo. *Advances in Virology*, 2010.

[2] MS Mustafa, V Rasotgi, S Jain, and Vl Gupta. Discovery of fifth serotype of dengue virus (denv-5): A new public health dilemma in dengue control. *Medical Journal Armed Forces India*, 71(1):67–70, 2015.

[3] Martina, Byron EE and Koraka, Penelope and Osterhaus, Albert DME. Dengue virus pathogenesis: an integrated view. *Clinical microbiology reviews*, 22(4):564–581, 2009.

[4] Dengue vaccine: Who position paper, september 2018 - recommendations. *WHO Report, Vaccine*, 2018.

[5] Nuraini, Nuning and Tasman, Hengki and Soewono, Edy and Sidarto, Kuntjoro Adji. A with-in host dengue infection model with immune response. *Mathematical and Computer Modelling*, 49(5-6):1148–1155, 2009.

[6] Thibodeaux, Jeremy J and Hennessey, Michael. A Within-Host Model of Dengue Infection with a Non-Constant Monocyte Production Rate. *Applied Mathematics*, 7 (18), 2016.

[7] Clapham, Hannah E and Quyen, Than Ha and Kien, Duong Thi Hue and Dorigatti, Ilaria and Simmons, Cameron P and Ferguson, Neil M. Modelling virus and antibody dynamics during dengue virus infection suggests a role for antibody in virus clearance. *PLoS computational biology*, 12(5), 2016.

[8] Clapham, Hannah E and Tricou, Vianney and Van Vinh Chau, Nguyen and Simmons, Cameron P and Ferguson, Neil M. Within-host viral dynamics of dengue serotype 1 infection. *Journal of the Royal Society Interface*, 11(96), 2014.

[9] Chahibi, Youssef and Akyildiz, Ian F. Molecular communication noise and capacity analysis for particulate drug delivery systems. *IEEE Transactions on Communications*, 62(11):3891–3903, 2014.

[10] Youssef Chahibi, Massimiliano Pierobon, and Ian F Akyildiz. Pharmacokinetic modeling and biodistribution estimation through the molecular communication paradigm. *IEEE Transactions on Biomedical Engineering*, 62(10):2410–2420, 2015.

[11] Abhay PS Rathore and AL St. John. Immune responses to dengue virus in the skin. *Open Biology*, 8(8), 2018.

[12] Cameron P Simmons, Kirsty McPherson, Nguyen Van Vinh Chau, DT Hoai Tam, Paul Young, Jason Mackenzie, and Bridget Wills. Recent advances in dengue pathogenesis and clinical management. *Vaccine*, 33(50):7061–7068, 2015.

[13] Rondina, Matthew T and Weyrich, Andrew S. Dengue virus pirates human platelets. *Blood*, 126(3):286–287, 2015.

[14] Sanders, Charles R. Biomolecular ligand-receptor binding studies: theory, practice, and analysis. *Nashville: Vanderbilt University*, pages 1–43, 2010.

[15] Izabela A Rodenhuis-Zybert, Jan Wilschut, and Jolanda M Smit. Dengue virus life cycle: viral and host factors modulating infectivity. *Cellular and Molecular Life Sciences*, 67(16):2773–2786, 2010.

[16] Arboleda, John F and Urcuqui-Inchima, Silvio. Vitamin D-regulated microRNAs: are they protective factors against dengue virus infection? *Advances in virology*, 2016.

[17] Screaton, Gavin and Mongkolsapaya, Juthathip and Yacoub, Sophie and Roberts, Catherine. New insights into the immunopathology and control of dengue virus infection. *Nature Reviews Immunology*, 15(12), 2015.

[18] Tuiskunen Bäck, Anne and Lundkvist, Åke. Dengue viruses–an overview. *Infection ecology & epidemiology*, 3(1), 2013.

[19] Pierson, Theodore C and Diamond, Michael S. Degrees of maturity: the complex structure and biology of flaviviruses. *Current opinion in virology*, 2(2):168–175, 2012.

[20] Han, Qing and Bradshaw, Elizabeth M and Nilsson, Björn and Hafler, David A and Love, J Christopher. Multidimensional analysis of the frequencies and rates of cytokine secretion from single cells by quantitative microengraving. *Lab on a chip*, 10(11):1391–1400, 2010.

[21] Bonin, Carla Rezende Barbosa and Fernandes, Guilherme Cortes and dos Santos, Rodrigo Weber and Lobosco, Marcelo. Mathematical modeling based on ordinary differential equations: A promising approach to vaccinology. *Human vaccines & immunotherapeutics*, 13(2):484–489, 2017.